Elsevier Editorial System(tm) for Chemical Geology

Manuscript Draft

Manuscript Number:

Title: The viscosity of shoshonitic melts (Vulcanello Peninsula, Aeolian Islands, Italy): insight on the magma ascent in dikes

Article Type: Research Article

Section/Category:

Keywords: shoshonite viscosity, water, falling sphere, micropenetration, volcanology, magma ascent in dikes, hazard

Corresponding Author: Dr guido ventura, Senior resercher PhD

Corresponding Author's Institution: Istituto Nazionale Geofisica Vulcanologia

First Author: Francesco Vetere

Order of Authors: Francesco Vetere; Harald Behrens; Valeria Misiti; Guido Ventura; Francois Holtz; Rosanna De Rosa; Joachim Deubener

Manuscript Region of Origin:

Abstract: The viscosity of shoshonitic melts from Vulcanello Peninsula (Vulcano Island, Italy) is experimentally determined at temperatures between 733 K and 1673 K. The water content of the melts varies from 0.03 to 4.75 wt% H2O. The micropenetration technique is employed at ambient pressure in the high viscosity range (109-1012 Pa*s). Falling sphere(s) experiments are performed at 500 and 2000 MPa in the low viscosity range (100.5-103 Pa*s). Results show a decrease of about 2 orders of magnitude in viscosity if ~ 3 wt% of water is added to the dry melt at 1300 K. At high temperature the viscosity of Vulcanello melts is intermediate between that of andesitic and basaltic melts. In contrast, at low temperatures (≤1050 K), the shoshonitic melt is characterized by a lower viscosity with respect to the two

previous melts. Based on our new data set, a calculation model is proposed to predict the viscosity of the shoshonitic melts as a function of temperature and water content. The viscosity data are used to constrain the ascent velocity of shoshonitic magmas from Vulcanello within dikes. Using petrological data (temperature and crystal content of the magma) and volcanological information (geometrical parameters of the eruptive fissure and depth of magma storage), we estimate the time scale for the ascent of magma from the main reservoir to the surface. Results show time scales in the order of hours to few days. We conclude that the rapid ascent of poorly evolved melts from Moho depths should be taken into account for the hazard assessment of Vulcano Island.

The viscosity of shoshonitic melts (Vulcanello Peninsula, Aeolian Islands, Italy): insight on the magma ascent in dikes

Francesco Vetere[1,2], Harald Behrens[3], Valeria Misiti[2], Guido Ventura[2*], Francois Holtz[3], Rosanna De Rosa[1], Joachim Deubener[4]

[1]Università della Calabria, Dipartimento Scienze della Terra, via P. Bucci I-87036 Arcavacata di Rende (CS), Italy

[2]Istituto Nazionale di Geofisica e Vulcanologia, Department of Seismology and Tectonophysics, via di Vigna Murata 605, I-00143 Roma, Italy

[3]Institut für Mineralogie, Leibniz Universität Hannover, Callinstr. 3, D-30167 Hannover, Germany

[4]Institute für Nichtmetallische Werkstoffe Technische Universität Claustal Zehntnerstr. 2a D-38678 Clausthal-Zellerfeld, Germany

[*]Corresponding author: Guido Ventura, Istituto Nazionale di Geofisica e Vulcanologia, Department of Seismology and Tectonophysics, via di Vigna Murata 605, I-00143 Roma, Italy. Phone: +39 06 51860221; Fax: +39 06 5041303; e-mail: ventura@ingv.it

Abstract The viscosity of shoshonitic melts from Vulcanello Peninsula (Vulcano Island, Italy) is experimentally determined at temperatures between 733 K and 1673 K. The water content of the melts varies from 0.03 to 4.75 wt% H_2O. The micropenetration technique is employed at ambient pressure in the high viscosity range (10^9-10^{12} Pa·s). Falling sphere(s) experiments are performed at 500 and 2000 MPa in the low viscosity range ($10^{0.5}$-10^3 Pa·s). Results show a decrease of about 2 orders of magnitude in viscosity if ~ 3 wt% of water is added to the dry melt at 1300 K. At high temperature the viscosity of Vulcanello melts is intermediate between that of andesitic and basaltic melts. In contrast, at low temperatures (≤1050 K), the shoshonitic melt is characterized by a lower viscosity with respect to the two previous melts. Based on our new data set, a calculation model is proposed to predict the viscosity of the shoshonitic melts as a function of temperature and water content. The viscosity data are used to constrain the ascent velocity of shoshonitic magmas from Vulcanello within dikes. Using petrological data (temperature and

crystal content of the magma) and volcanological information (geometrical parameters of the eruptive fissure and depth of magma storage), we estimate the time scale for the ascent of magma from the main reservoir to the surface. Results show time scales in the order of hours to few days. We conclude that the rapid ascent of poorly evolved melts from Moho depths should be taken into account for the hazard assessment of Vulcano Island.

Keywords: shoshonite viscosity, water, falling sphere, micropenetration, volcanology, magma ascent in dikes, hazard

1. Introduction

Viscosity is an important factor governing both intrusive and volcanic processes. Since the pioneering study of Bowen (1934), an intensive work has been devoted to viscosity determination for melts varying from felsic to mafic compositions. Techniques applied in the high viscosity range (10^8 to 10^{13} Pa·s) include micropenetration (e.g., Hess and Dingwell, 1996), parallel plate viscosimetry (e.g., Richet et al., 1996; Whittington et al., 2000) and the evaluation of kinetics of interconversion of hydrous species (Zhang et al., 2003). In the low viscosity range (0.1-10^4 Pa·s), the falling sphere technique is the only established method for viscosity determinations at elevated pressures (e.g., Shaw, 1963). Indirect constraints on viscosity may be obtained from the diffusivity of network former using the Eyring relationship (Chakraborty, 1995).

The main parameters that govern the viscosity of silicate melts are the bulk composition of the melt and the temperature (e.g., Bottinga and Weill, 1972; Shaw, 1972). Pressure has only little effect at crustal depths (below about 800 MPa) (Kushiro et al., 1976; Behrens and Schulze, 2003), whereas crystals (Lejeune and Richet, 1995; Bouhifd et al, 2004; Sato 2005) and bubbles (Lejeune et al., 1999) may have an important influence. Among the compositional parameters,

the water content of the melt is of particular importance (e.g. Schulze et al. 1996, Whittington et al. 2000). Due to difficulties in the measurement of low viscosity melts with the falling sphere techniques, silicic (i.e. rhyolitic) melts have been more intensively investigated than basaltic ones (Shaw 1963, Hess and Dingwell 1996, Schulze et al.1996, Holtz et al. 1999, Romano et al 2001 and reference therein).

Most studies have concentrated either on the prediction of the effect of anhydrous melt composition on viscosity (e.g., Russell et al 2003, Giordano and Dingwell 2003a) or on the effect of dissolved water for specific anhydrous compositions (e.g., for rhyolite, see model of Hess and Dingwell, 1996; for andesite see model of Vetere et al. 2007). Although progress has been made in modelling the viscosity as a function of water content and bulk composition, the prediction of viscosity for a composition which was not experimentally investigated has still large uncertainty (Misiti et al. 2006; Hui and Zhang 2007, Vetere et al 2007).

Up to now, viscosity data for hydrous and anhydrous shoshonitic compositions are lacking. In this study, viscosity determinations are performed on a re-melted natural shoshonite from Vulcanello Peninsula (Vulcano Island; Aeolian Islands, Italy). Various amounts of water are added to probe the effect of H_2O on melt viscosity. The data are compared with other mafic and alkali-rich compositions such as basalts (Giordano and Dingwell 2003b), trachytes (Misiti et al. 2006) and andesites (Vetere et al. 2007). The new data are used to investigate the time scale of magma ascent in this area of Aeolians.

2. Geological and volcanological setting

Vulcano is the southernmost island of the Aeolian Archipelago, and, with Lipari and Salina, it is located along a NNW-SSE–trending strike-slip fault system (Ventura et al., 1999). The activity on Vulcano dates back to about 120 ka (De Astis et al., 1997). The island is formed by Primordial Vulcano and Piano Caldera in the south, and by Mastro Minico–Lentia complex

and Fossa Caldera in the north (**Fig. 1a**). The active Fossa Cone is located within the Fossa Caldera. Last eruption was in 1888/1890. The small lava shield and pyroclastic cones of Vulcanello (123 m a.s.l.) form the northern part of the island (**Fig. 1b**). Based on greek and latin writing (e.g., Strabo in the *Geography*), Vulcanello has been traditionally dated to 183 or 126 BC. However, recent archeomagnetic studies postdate the building of Vulcanello to AD 1000 and 1600 (Arrighi et al., 2006) and confirm the hypothesis that its "birth" was related to a long-lived eruptive period. The oldest products are those of the pyroclastic cone of Vulcanello I (AD 1050) (Fig. 1b). The shield lava (tholoid) and the cone II were built through a continuous activity between AD 1100 and 1250. The lava flows were emitted from a 600 m long, 0.5 to 1.5 m wide, NE-SW striking fissure. These flows consist of shoshonites and minor latites and, together with the volcanic rocks from La Fossa Cone, are the most alkaline products of the Aeolian Arc. Following Peccerillo et al. (2006), the shoshonites of Vulcanello represent basaltic magmas that slightly evolve at the mantle-continental crust interface (20 km depth) and rapidly upraise to the surface. The new archeomagnetic data suggest an age of AD1600 for the cone III eruption and the final trachytic flow (Arrighi et al., 2006 and references therein).

3. Experimental and analytical methods

3.1 Starting material

As reported by Keller (1980) Vulcanello is mainly composed by *tephrytic leucite* lavas. Based on Total Alkali-Silica (TAS) the Vulcanello magmas fall in the shoshonitic field (table 1; De Astis et al., 1997). For the viscosity study we used a porphiritic sample from a lava fountain of the early phase of activity whose composition matches very closely that of the shield lavas. The modal abundance of phenocrysts is 8-11 vol.%. The mineral phases are clinopyroxenes (Cpx),

plagioclases (Pl) and amphiboles (Amph). The phenocrysts often contain inclusions of Fe-Ti oxides. The groundmass consists of glass, leucite (Lc), Fe-Ti oxides, Cpx, Pl, Amph, and small amount of olivine (Ol). The bulk rock is characterized by SiO_2 = 53.47 wt.% and $Na_2O + K_2O$ = 8.38 wt.% and is representative for the average composition of the Vulcanello lavas (De Astis et al., 1997) (composition Vul1, **Tab. 1**).

About 100 g of crushed bulk rock was melted in a Pt crucible in air at 1873 K for 4 hour. After quenching on a metal plate, the obtained glass was crushed and melted again in the same furnace at the same conditions to improve homogeneity. The composition of several glass fragments was analyzed by electron microprobe CAMECA SX 100. Measurement conditions were: defocused beam of 15 µm diameter, accelerating voltage of 15 kV and a beam current of 4 nA.

The procedure to synthesize water-bearing glasses is described in detail by Vetere et al. (2006). Distilled water was added stepwise to a dry glass powder in AuPd capsules (diameter of 5-6 mm, length of 30-40 mm). After welding, the capsules were placed in an internally heated gas pressure vessel (IHPV) at 1523 K and 500 MPa for 24 hours. The syntheses were terminated by rapid quench (see Berndt et al. 2002 for experimental details).

For the viscosity experiments performed in IHPVs, cylinders (diameter: 3 - 6 mm; length: 10 – 15 mm) were cored out of the hydrous glasses. The residual glass was crushed to a fine grained powder except for some fragments to be used for determination of the water content and the Fe^{2+}/Fe_{tot} ratio. The preparation of capsules for the high pressure viscosity experiments is detailed in Vetere et al. (2006).

Samples were not pre-equilibrated for experiments in a piston cylinder apparatus (PCA), but used as received after melting at ambient pressure (nominally dry glasses) or after synthesis in the IHPV (hydrous glasses containing about 2 wt % H_2O, samples Vul 24, Vul 25, Vul 27, Vul

28, see Table 2). Preparation of capsules for falling sphere experiments in the PCA was done in same way as described in Misiti et al. (2006).

3.2 Iron and water determination

The Fe^{2+}/Fe_{tot} ratio in glasses was measured before and after the experiments (see Table 2) by using a modified colorimetric method (Wilson 1960, Vetere et al 2007). Compared to the starting glass (Fe^{2+}/Fe_{tot} = 0.40**, Tab. 1**) the glasses after high pressure syntheses in the IHPV are more reduced (Fe^{2+}/Fe_{tot} of 0.55 – 0.75**, Tab. 2**As shown by Vetere et al. (2007) for an andesitic composition, the Fe^{2+}/Fe_{tot} can influence the viscosity by about 0.2 log units in dry melts. This difference becomes less pronounced for water-rich samples. In this study, the Fe^{2+}/Fe_{tot} ratio of glasses determined before and after the viscosity determinations do not show evidence for changing Fe^{2+}/Fe_{tot} ratio during the viscosity experiments (Tab. 2).

The water content of the glasses was measured by Karl-Fischer Titration (KFT) and infrared spectroscopy (IR). To account for unextracted water contents measured by KFT, the values obtained after extraction (KFT) were corrected by adding 0.13 wt% H_2O (Behrens and Stuke, 2003). The uncertainty of the KFT analysis is estimated to be ± 0.10 wt%, including the uncertainty due to unextracted water and the error in the titration rate (for details of the analytical technique and error estimation see Behrens and Stuke, 2003). To test the homogeneity of H_2O concentrations in selected samples, wafers from different part of the samples were analyzed by KFT (Table 2).

Infrared spectroscopy was employed to determine the water content of the nominally anhydrous melts and to analyzed possible dehydration and sample alteration during micropenetration experiments. Absorption spectra of selected samples were recorded on double-

side polished thin sections (thickness mm) using an IR microscope IRscopeII which is connected to an FTIR spectrometer Bruker IFS88. Measurements were performed in the mid-infrared using a globar light source, a KBr beam splitter and a narrow range MCT detector. The analyzed area was limited by a slit aperture between objective and detector to ca. 100 x 100 µm in the focus plane. Typically 50 scans were accumulated for each spectrum with a spectral resolution of 2 cm^{-1}. The water content was derived from the baseline-corrected height of the band at 3550 cm^{-1} employing a molar absorption coefficient of 73 ± 5 L mol^{-1} cm^{-1} derived from a shoshonitic glass containing 2.11 wt% H_2O (measured by KFT).

3.3 Falling sphere methods

Viscosity was measured in the high temperature range using the falling sphere method. Experiments at 500 MPa were carried out at temperatures from 1373 to 1673 K in internally heated pressure vessels (IHPVs) at the Institute of Mineralogy, University of Hannover (Germany). The samples were first pressurized and then heated up using two different heating rates: 30K/min to 1073K and 100K/min to the final temperature. After a dwell of 287 to 3645 s the capsule containing the viscosity sample was rapidly quenched (estimated quench rate of 150-200 K/s, Berndt et al., 2002).

Two experiments with nominally dry samples were performed at 2000 MPa, at 1473 and 1573 K, in a ¾ inch end-load piston cylinder apparatus (~~PCA;~~ Voggenreiter company) at the Istituto Nazionale di Geofisica e Vulcanologia in Rome (Italy) to determine the effect of pressure on melt viscosity. Additional experiments were also done in the PCA at 500 MPa. The dry capsules were stored in an oven at 110 °C overnight to remove humidity and then welded. Loaded capsules were put into 19.1 mm NaCl-crushable alumina-pyrex (nominally anhydrous

samples) or NaCl-crushable alumina-pyrophillite-pyrex (Freda et al., 2001) assemblies. The first assemblage is used for dry conditions; as suggested by Freda et al (2001) the second assemblage is preferable for H_2O-bearing samples to avoid water loss during experiments.

The samples were first pressurized using the piston-in technique, and then heated at a rate of 200 K/min up to 20 K below the target temperature. A smaller rate of 40 K/min was applied within the last 20 K of heating to avoid overshooting. Temperature was controlled within ±3 K using one $W_{95}Re_5$-$W_{74}Re_{26}$ (type C) thermocouple located close to the centre of the sample (for further details see Misiti et al., 2006). The experiments were ended by switching off the heating power while maintaining pressure constant by automatic compensation. The initial quench rate was about 2000 K/min.

Because the Fe-bearing glasses are not transparent, we used X-ray images to monitor sphere positions (SIEMENS HELIODENT DS X-rays camera, exposure time of 0.16 s in Hannover (Vetere et al 2007); de Götzen xgenus ® dc camera with digital scanning image, exposure time of 0.20 s in Rome (Misiti et al 2006)). X-ray radiographs of each sample were recorded before and after the experiments for two different orientations of the sample (perpendicular to each other) to measure the positions of the sphere relative to the Pt marker and relative to the capsule walls. The settling distance of the sphere could be measured (with an error of ±20 μm) by superimposing pre- and post-experiments images (for details, see Misiti et al. 2006).

The viscosity η is calculated by Stokes law

$$\eta = \frac{2 \cdot t \cdot g \cdot \Delta\rho \cdot r^2 \cdot C_F}{9 \cdot d} \qquad (1)$$

where d is the settling distance in cm, t is the run duration in sec, $\Delta\rho$ is the density difference between the sphere and the melt, g is the acceleration due to gravity (9.81 m/s^2), r is the radius of the sphere and C_F is the Faxen correction (Faxen, 1923) which accounts for the effect of viscous drag by the capsule wall on the settling sphere. To account for movement of spheres during

heating and cooling, we calculated the effective run duration for each experiment as described in Vetere et al. (2006). Room temperature densities of Pt and Pd are 21.45 and 12.02 g/cm^3, respectively. No correction was made for differential compression and thermal expansion of the solid materials because this would contribute less than 1% to the viscosity. The sphere radius was measured before the experiments and it was not possible to check whether a possible change in shape happened during pressurization.

The density of the dry glass was measured by weighing single glass pieces in air and in water. The average value from 3 measurements is 2.656 g/L. According to Richet et al. (2000) the partial molar volume of H_2O in glass is 12.0 cm^3/mol and considering that the pressure derivative is roughly 1% per 500 MPa for silicate glasses (Mysen and Richet 2005)we derived the following we derived the following equation to estimate the density of the run product.

$$density\ (\text{g/L}) = (2658 - 19.7 \cdot C_{H2Ot}) \cdot (1 + 0.00002 \cdot P) \qquad (2)$$

with C_{H2Ot} in wt% and P in MPa.

3.4 Micropenetration technique

Indentation measurements were performed at ambient pressure on a vertical dilatometer (Bähr VIS 404) at the Institute fur Nichtmetallische Werkstoffe, Technische Universitat Clausthal (Germany). Cylindrical plates (diameter: 4-5 mm; height: 1.5 mm) with coplanar polished base planes were heated up to the desired temperature at a rate of 10 K/min. After stabilization of temperature a load of 0.5 – 0.9 kg was placed on top of a pushing rod which pressed a sapphire micro-sphere (radius R = 0.75 mm) into the glass surface. Indentation of the sphere into the sample was measured as a function of time using a linear variable displacement transducer. The shear viscosity η was calculated as

$$\eta = \frac{0.1875 \cdot F \cdot t}{\sqrt{R}\sqrt{L^3}} \quad (3)$$

where F is the applied force (= mass of load times gravitation acceleration), t is the time, R is the radius of the sphere, and L is the indentation depth (Douglas et al 1965; Brückner and Demharter 1975). The accessible viscosity range of the apparatus is 10^8 – $10^{14.7}$ Pa·s (Zietka et al., in press). The system was calibrated by the standard glass G1 of the Physikalisch-Technische Bundesanstalt (PTB, Böse et al., 2001). The standard deviation of the viscosity was ± 0.2 log units at $10^{14.7}$ Pa s and ±0.1 log units at 10^{12} Pas.

Experimental temperature varied between 893 K and 1003 K for nominally dry melts while for the hydrous ones the temperature cover a range from 733 to 823 K. Accuracy of temperature was within ± 6 K, limited by the accuracy of the thermocouples and the measuring equipment (Zietka et al., in press).

4. Results

4.1 Falling sphere

Results of the falling sphere experiments are summarized in Table 2. Falling sphere experiments cover a range of temperature from 1373 to 1623 K and water content from nominally dry to 4.75 wt% H_2O. The minimum viscosity measured (sample Vul 13b) was 5.6 Pa·s using Pt sphere with a radius of 62.5 μm,~ 5 min run time, temperature of 1523 K and pressure of 500 MPa. Viscosity experiments with dry melts were possible only at temperatures from 1573 to 1673 K (Vul 21, Vul 22, Vul 23a and Vul 23b). In one case (samples Vul23a and Vul23b, Table 2) we performed two viscosity experiments keeping the same condition of T and P, varying the run time and the size of spheres. Two identical capsules were prepared for PCA runs. The Pt spheres used were 95 and

125 μm in radius for samples Vul23a and Vul23b, respectively. After welding shut the capsules, two separate runs with a dwell time of 729 and 1828 s, respectively, were performed (Table 2). The viscosities derived from these experiments agree within the estimated error, demonstrating the reliability of the falling sphere experiments. The effect of pressure was tested for the nominally dry melt at 1573 K (500 MPa: samples Vul23a and Vul23b; 2000 MPa: sample Vul7). Results show no dependence of viscosity on pressure in this range; the viscosity at 2000 MPa is slightly higher than that at 500 MPa (Table 2) but the two values are identical within error.

The water contents measured before and after experiments on selected samples, are identical within error. Oxidation state of iron before and after the experiment in the IHPV shows no significant difference, due to the relatively short run time and due to the long term pre-equilibration of the melt in the same vessel. The effect of pre-equilibration is visible also in the decrease of Fe^{2+}/Fe_{tot} with increasing water content. At constant hydrogen fugacity in the vessel, the oxygen fugacity increases with water fugacity (water content of the melt). Dry samples processed in the PCA apparatus show a Fe^{2+}/Fe_{tot} ratio about 0.15 higher than the starting material (compare Tab. 1 and Tab. 2).

4.2 Partially crystallized samples

Samples obtained at 1473 K and 500 and 2000 MPa in nominally dry samples are below the liquidus temperature (**Fig. 2**). The size of the crystals is very small (1-5 μm) and it was not possible to analyse them quantitatively. In these samples the viscosity determined by the falling sphere technique is higher than expected, mainly due to the presence of crystals. The extrapolated viscosity for the pure melt at 1473 K is approximately $10^{2.7}$ Pa.s, while the average viscosity in partially crystallized samples at 1473 K and 500 MPa (Vul 3, Vul 4, Vul 5 and Vul 6, Table 2) is $10^{3.0}$ Pa.s. These samples have an amount of crystals of about 11 vol% (determined by standard

image processing technique, see Fig. 2). The crystal content of a sample obtained after an experiment at 1473 K and 2000 MPa pressure was even higher (~24 vol%, see Fig.2). Due to the relatively high crystals content, the short dwell time (half hour) and probably the small radius of the sphere, it was not possible to measure the viscosity in the first run. The experiment was repeated choosing a dwell time of about 1 hour (see Table 2 sample Vul 8), and a Pt sphere of 175 μm in radius (~ double respect to the previous sphere), allowing us to measure the viscosity of the partly crystallized sample.

The observed changes of viscosity by partial crystallization can be compared with the prediction of the Einstein-Roscoe equation (Einstein 1911, Roscoe 1952):

$$\eta = \eta_m \cdot (1 - \phi/0.6)^{-2.5} \qquad (4)$$

where η is the effective viscosity of a liquid with a volume fraction ϕ of crystals, and η_m is the viscosity of the melt. A value of $10^{2.98}$ Pa.s is calculated for the samples containing 11 vol.% crystals at 1473 K, 500 MPa (by setting the critical fraction of crystals at 0.6; Einstein 1911, Marsh 1981), close to the experimental value. For the higher crystal content of 24 vol%, the measured viscosity (Table 2) is ~0.75 log unit higher than that extrapolated for the pure melt and about 0.20 log unit higher than predicted by the Einstein-Roscoe equation.

4.3 Micropenetration experiments

In Fig. 4 a typical result of an indentation measurement is shown. Noteworthy, the derived viscosity values increase continuously with time at constant temperature. A possible explanation is the onset of sample alteration, e.g. crystallization of Fe-Ti-oxides as observed in viscosity experiments with andesites (Richet et al. 1996; Liebske et al. 2003, Vetere et al 2007). The increase in viscosity was less than 0.1 log units within the time interval used for measurement.

Thus we decided to use the average viscosity in that time interval as an estimate of the viscosity of supercooled shoshonitic melts, but we are aware that this value represents only a maximum viscosity.

Experiments were carried out with samples containing between 0.02 and 2.11 wt% H_2O.Results of the high viscosity experiments are reported in Table 3. The viscosity of the nominally dry and hydrous samples (0.02 and 2.11 wt% H_2O) shows a nearly Arrhenian behaviour in the temperature range 733 - 1003 K (**Fig. 4**). With the nominally anhydrous sample Vul y_1 two measurements were performed during the experimental sequence. With the sample Vul y_2 three temperature where investigated and the results are in agreement with those obtained with the previous one as illustrated in Fig. 4. In case of the hydrous sample Vul 14 the last measurement was performed at a temperature intermediate between those of the first two measurements. The consistency of the data (nearly Arrhenian behavior) implies that sample alteration had only minor effects on melt viscosity (less than 0.2 log units).

After experiments, samples Vul y_1 and Vul 14 were still clear glasses without visible crystallization (checked by microscopy). Sample Vul y_2 which was processed at higher temperature than Vul y_1 was much darker, indicating changes in iron environment and onset of crystallization of iron oxides (Liebske et al. 2003). But the consistence of viscosity data for both samples (Fig. 3) implies that crystals in the dry glasses (if present) had no significant influence on the measured viscosity and hence we used all the data presented in Tab. 3 to model the viscosity of shoshonitic melts. Water contents measured by IR spectroscopy are identical for the centre and the rim of the hydrous glass Vul14. Thus possible dehydration of the glass during the micropenetration experiment is limited to a zone < 20μm from the surface.

4.4 Vulcanello melts: a viscosity model.

The new viscosity dataset on a shoshonitic melt was used to develop an empirical model predicting the relative viscosity variation as a function of melt water content and temperature at geological relevant conditions. The data base consists of 24 measurements. The model is based on the VFT approach to account for the non-Arrhenian temperature dependence of viscosity. Data were fitted using a non-linear least-square regression. The following equation was found to best reproduce the experimental data and the observed viscosity trends:

$$\log\eta = -6.17 + \frac{7882.34}{(T-246.62)} + \frac{2366.04}{(T-534.21)} \cdot \exp\left(-474.96 \cdot \frac{w}{T}\right) \qquad (5)$$

where η is the viscosity in Pa·s, T the temperature in K and w is the water content in wt% H_2O. This equation reproduces the experimental data with a 1σ standard deviation of 0.17 log units (**Fig. 5**). Because of the lack of experimental data in the high viscosity range, this equation should be limited viscosity values below 10^{13} Pa s. It is also emphasized that the equation is not constrained for water contents above 2.1 wt% in the high viscosity regime. Based on Eqn. (5), the viscosity of the Vulcanello anhydrous melts at temperatures relevant for magmatic processes (1473 K$\leq T \leq$1273 K) varies between $6 \cdot 10^2$ Pa s and $5.1 \cdot 10^4$ Pa s. Within the same temperature range, melts with 2.0 wt.% H_2O have viscosities between 38 Pa s and 10^3 Pa s. Therefore, the viscosity of such hydrous melts is lower by nearly two orders of magnitude compared to the dry melts.

5. Discussion and conclusions

5.1 Comparison with previous data on depolymerized natural melts

Equation (5) allows us to compare the viscosity of shoshonitic melts with that of basaltic, andesitic and trachytic melts (Giordano et al., 2003b; Misiti et al., 2006; Vetere et al., 2007). At T>1050 K, the Vulcanello shoshonitic melt shows viscosity values between those of basalts and andesites (**Fig. 6**). This behavior can be expected taking into account that shoshonites have a SiO_2 content higher than that of basalts and lower than andesites (Table 1; Fig. 6), although the amount of alkali is higher than that of basalts and andesites. At T~1050 K, the viscosity of shoshonitic melt is close to that of basalts. Since anhydrous basaltic and shoshonitic systems are below the solidus temperature at 1050 K, the viscosity of anhydrous shoshonitic melts should always be higher than that of anhydrous basalts at equilibrium conditions. The viscosity difference between shoshonitic and trachytic melts increases with increasing temperature, reaching a maximum of about 2 log units at T>1400 K (Fig. 6). Following the model of Misiti et al. (2006), this difference decreases by increasing the water content dissolved in the melts.

5.2 Ascent of the Vulcanello shohonitic magma

The Vulcanello lava shield formed by effusions from a 600 m long, 0.5 to 1.5 m wide eruptive fissure (dike) (see section 2). Assuming that the magma upraise is due to buoyancy, the overpressure ΔP at the Moho depth, which is the depth at which the primary melts stay and differentiate (Zanon et al. 2003, Peccerillo et al. 2006) may be estimated using the relation:

$$\Delta P = \Delta\rho \cdot g \cdot h \qquad (6)$$

where $\Delta\rho$ is the difference between the density of the country rock and the melt, g is the gravity, and h is the vertical length of the dike. We select h = 20 km, which is the Moho depth below

Vulcanello (Ventura et al., 1999), and $\Delta\rho$ = 350 kg/m^3. This latter value is the difference between 2850 kg/m^3, which is the seismically and gravity constrained average density of the crustal rocks below the Aeolians (Cella et al., 2006), and the density of the Vulcanello shoshonitic melts (ρ=2500$\pm$100 kg/m^3). Using relation (6), we obtain 68 MPa, which is a value consistent with that estimated for other dike systems, e.g. the 60 MPa source overpressure estimated by Menard and Tait (2002) at the McKenzie swarm (Canada). The above estimated value of ΔP for the opening of the Vulcanello dike allows us to have a semiquantitative estimate the Reynolds number *Re* within the dike. It is well known that a laminar flow regime occurs at $Re \leq 10$, whereas a turbulent flow regime occurs at $Re \geq 1000$. Transitional regimes are characterized by $10 < Re \leq 1000$. A critical value of the viscosity η_c between these regimes can be estimated if ΔP, the width of the dike *w,* and *h* are known throughout the relation (Sparks et al., 2006):

$$\eta_c = [(2\Delta P \rho w^3)/(3h\, Re_c)]^{1/2} \qquad (7)$$

where Re_c is the critical *Re*. Turbulent flow occurs when $\eta < \eta_c$. In the equation (7), we adopted the following values: ΔP=68 MPa (equation 6), ρ=2500 kg/m^3, *h*=20 km, and *w*=1 m, i.e. the average value of the Vulcanello dikes. We also select 10 and 1000 as values representative for Re_c. For Re_c=10, we obtain η_c=238 Pa s. For Re_c=1000, η_c is 23 Pa s. Using equation (5) and taking into account that the temperature estimated for the Vulcanello magmas is 1353$\pm$40 K (Zanon et al., 2003), a viscosity of $10^{3.8}$ Pa s for a dry melt and of $10^{2.4}$ Pas for a melt containing 2.0 wt.% H_2O can be estimated. Moreover, taking into account that the Vulcanello shoshonites have a crystal content of about 10 vol.%, we obtain, using the Einstein-Roscoe equation, a viscosity of $10^{4.0}$ Pa s for the dry magma and of $10^{2.6}$ Pa s for the hydrous (H_2O=2.0 wt.%) magma. These viscosity values are in the same order of magnitude than those estimated using eq. (7) for Re_c =10. We conclude that the Vulcanello magma moved within the dike in a prevailing

laminar flow regime. To calculate the ascent velocity u of such a magma we use the relation of Lister and Kerr (1991) for laminar flows:

$$u=(w^2/3\cdot\eta)\Delta\rho\cdot g \quad (8)$$

by setting w=1 m, $\Delta\rho$=350 kg/m^3, η(dry)= $10^{4.0}$ Pa s, and η(hydrous)= $10^{2.6}$ Pa s, we obtain the following values: u(dry)=0.11 m/s, and u(hydrous)=2.87 m/s. A lower limit for the ascent velocity of the shoshonitic magmas can be estimated by applying the Stokes law to the cm- to dm-sized quartz xenoliths with preserved high-pressure fluid inclusions occurring at Vulcanello (Zanon et al., 2003). Assuming a Newtonian rheology, the settling velocity u_s is:

$$u_s=C_d\cdot(\Delta\alpha\cdot g\cdot d/\rho)^{1/2} \quad (9)$$

where C_d is the drag coefficient (~1), $\Delta\alpha$ is the density contrast between the xenolith and the magma, d is the xenolith diameter, and ρ is the magma density. By setting d=0.1 m and quartz density = 2650 kg/m^3, the settling velocity is 0.24 m/s. Therefore, by selecting 0.24 m/s and 2.87 m/s as representative values of the lowest and highest velocity, the ascent time (h/u) of the Vulcanello magmas is between ~ 2 h and 23 h (~1 day). The velocity values of the Vulcanello shoshonites are one to two order of magnitude higher than those estimated for Na-alkaline magmas (e.g. the Ustica basalts (u~0.01 m/s); Alletti et al., 2005) and lower than those estimated for kimberlites (u=2.9-16.8 m/s; Sparks et al., 2006). The ascent velocities of shoshonites are within the same order of magnitude of those estimated for the Kilauea basalts (u up to 1.4 m/s; Klein et al. 1987) and East of Izu Peninsula (u~0.3 m/s; Hayashi and Morita, 2003). Taking into account that the models (equations 7 to 9) used to calculate the ascent velocity of the Vulcanello magmas does not consider the possible role of (1) the volatile exolution, which can cause a viscosity increase in the magma at the tip of the dyke, (2) freezing processes at the walls, which also can locally increase the viscosity (Wylie et al., 1999), and (3) the constant geometry of the dike in depth, the our velocity estimates must be considered as indicating an order of magnitude

rather than being absolute values. Additional analytical and experimental studies to constrain pre-eruptive temperatures, volatile contents and degassing processes during ascent at Vulcanello would be helpful to quantify the physical parameters of magmas. In addition, more information from geophysical data must be collected in future studies to better constraints the dike geometry in depth, even if numerical models on the ascent of magma in dikes with varying shape show that the dike geometry plays a major role in controlling the mass flux but do not significantly affect the average ascent velocity Giberti and Wilson (1990). In any case, our data suggest that the 20 km ascent may have occurred within hours to a few days. This is consistent with the observation that, at Vulcano, the eruptions triggered by the sudden arrival of shoshonitic magmas from a deep (~20 km) reservoir did not show significant long to medium term precursory signals (Peccerillo et al., 2006). We conclude that the hazard evaluation at Vulcano Island should consider the rapid ascent of less evolved melts from depths close to the Moho and not only the upraise of evolved magma from shallow chambers.

Acknowledgements. This research was funded by the Italian Dipartimento della Protezione Civile in the frame of the 2004-2006 agreement with Istituto Nazionale Geofisica e Vulcanologia-INGV and by DFG project Ho 1337/16. We thank Otto Diedrich, Willi Hurkuck, Bettina Aichinger, Piergiorgio Scarlato and Lilli Freda for the experimental and logistic support.

References

Alletti, M., Pompilio, M., Rotolo, S., 2005. Mafic and ultramafic enclaves in Ustica Island lavas: inferences on composition of lower crust and deep magmatic processes. Lithos, 84, 151-167.

Arrighi S., Tanguy, J., Rosi, M., 2006. Eruptions of the last 2200 years at Vulcano and Vulcanello (AeolianIslands, Italy) dated by high-accuracy archeomagnetism. Physics of the Earth and Planetary Interiors, 159, 225-233.

Behrens, H., Schulze, F., 2003. Pressure dependence of melt viscosity in the system $NaAlSi_3O_8$-$CaMgSi_2O_6$. American Mineralogist 88, 1351-1363.

Berndt, J., Liebske, C., Holtz, F., Freise, M., Nowak, M., Ziegenbein, D., Hurkuck, W., Koepke J., 2002. A combined rapid-quench and H_2-membrane setup for internally heated pressure vessels: description and application for water solubility in basaltic melts. American Mineralogist 87, 1717-1726.

Bottinga, Y., Weill, D.F., 1972. Viscosity of Magmatic Silicate Liquids - Model for Calculation. American Journal of Science 272, 438-475.

Bouhifd, M.A., Richet, P., Besson, P., Roskosz, M., Ingrin, J. , 2004. Redox state, microstructure and viscosity of a partially crystallized basalt melt. Earth and Planetary Science Letters 218, 31-44.

Bowen N.L., 1934. Viscosity data for silicate melts. Transaction of the American Geophysical Union, 15th annual meeting, 249-255.

Brückner R., Demharter G.,1975. Systematische Untersuchungen über die Anwendbarkeit von Penetrationsviskosimetern, Glastech. Ber. 48, 12-18.

Chakraborty, S., 1995. Diffusion in silicate melts Structure, Dynamics and Properties of Silicate Melts. Reviews in Mineralogy, 32, 411-503.

Cella, F., de Lorenzo, S., Fedi, M., Loddo, M., Monelli, F., Rampolla, A., Zito, G., 2006. Temperature and density of the Tyrrhenian lithosphere and slab and new interpretation of gravity field in the Thyrrhenian Basin. Tectonophysics, 412, 27-47.

Chen, H.C., De Paolo, D.J., Nakada, S., Shieh, Y.M., 1993. Relationship between eruption volume and neodymic isotopic composition at Unzen volcano. Nature, 362, 831-834.

De Astis, G.F., La Volpe, L., Peccerillo, A., Civetta, L., 1997. Volcanological and petrologicalevolution of the Vulcano Island (Aeolian Arc,Southern Tyrrhenian Sea):

Journal of Geophysical Research 102, 8021–8050.

Douglas R.W. Amstrong W.L, Edward J.P., Hall D., 1965. A penetration viscometer. Glass Technology 6, 52-55.

Einstein, A., 1911. Eine neue Bestimmung der molekuldimensionen. Annals of Physics, 19, 289-306.

Faxen, H., 1923. Die Bewegung einer starren Kugel längs der Achse eines mit zäher Flüssigkeit gefüllten Rohres. Ark. Math., Astro Fysik, 17, 1-28 (in German).

Freda, C., Baker, D.R., Ottolini, L., 2001. Reduction of water loss from gold-palladium capsules during piston-cylinder experiments by use of pyrophyllite powder. American Mineralogist 86, 234-237.

Giberti, G., Wilson, L., 1990. The influence of geometry on the ascent of magma in open fissures. Bulletin of Volcanology 52, 515-521.

Giordano, D., Dingwell, D.B., 2003a. Non-Arrhenian multicomponent melt viscosity: a model. Earth Planetary Science Letters 208, 337-349.

Giordano, D., Dingwell, D.B., 2003b. Viscosity of hydrous Etna basalt: implication for Plinian-style basaltic eruption. Bulletin of Volcanology 65, 8-14.

Hayashi, Y. & Morita, Y. (2003) An image of a magma intrusion process inferred from precise hypocentral migrations of the earthquake swarm east of the Izu Peninsula. Geophysical Journal International 153 (1), 159-174.

Hess, K.U., Dingwell, D.B., 1996. Viscosities of hydrous leucogranitic melts: A non-Arrhenian model. American Mineralogist 81, 1297-1300.

Holtz, F., Roux, J., Ohlhorst, S., Behrens, H., Schulze, F., 1999. The effects of silica and water on the viscosity of hydrous quartzofeldspathic melts. American Mineralogist 84, 27-36.

Huy, H., and Zhang, Y., 2007. Toward a general viscosity equation for natural anhydrous and hydrous silicate melts. Geochimica et Cosmochimica Acta 71, 403-416.

Keller, 1980. The island of Vulcano. Rend. Soc. Italian Miner. Petrol.36, 369–414.

Klein F.W., Koyanagi R.Y., Nakata J.S., Tanigawa W.R., 1987. The seismicity of Kilauea's magma system. U.S. Geological Survey 1350, 1019-1185.

Kushiro, I., Yoder, H.S., Mysen, B.O., 1976. Viscosities of basalt and andesite melts at high pressures. Journal of Geophysical Research 81, 6351-6356.

Lejeune, A.M., Richet, P., 1995. Rheology of crystal-bearing silicate melts - an experimental study at high viscosities. Journal of Geophysical Research: Solid Earth 100, 4215-4229.

Lejeune, A.M., Bottinga, Y., Trull, T.W., Richet, P., 1999. Rheology of bubble-bearing magmas.

Earth Planetary Science Letters 166, 71-84.

Liebske, C., Behrens, H., Holtz, F., Lange, R.A., 2003. The influence of pressure and composition on the viscosity of andesitic melts. Geochimica et Cosmochimica Acta 67, 473-485.

Lister, J.R., and Kerr, R.C., 1991. Fluid-Mchanical models of crack propagation and their application to magma transport an dyke. Journal of Geophysical Research 96, 10049-10077.

Marsh, B.D., 1981. On the crystallinity, probably occurrence, and rheology of lava and magma. Contributions to Mineralogy and Petrology 78, 85-98.

Menand, T., Tait, S.R., 2002. The propagation of a buoyant liquid filled fissure from a source under constant pressure: an experimental approach. Journal of Geophysical Research 107, 2306: 16-1-14.

Misiti V., Freda, C., taddeucci, J., Romano, C., Scarlato, P., Longo, A., Papale, P., Poe, B.T., 2006. the effect of H_2O on the viscosity of K-trachytic melts at magmatic temperatures. Chemical Geology 35, 124-137.

Mysen, B. Richet, P., 2005. Silicate Glasses and Melts - Properties and Structure. Developments in Geochemistry 10, Elsevier Amsterdam, pp 544.

Peccerillo, A., Frezzotti, M.L., De Astis, G., Ventura, G., 2006. Modeling the magma plumbing system of Vulcano (aeolian Island, Italy) by integratine fluid-inclusion geobarometry, petrology and geophysics. Geology, 34, 17-20.

Richet, P., Lejeune, A.M., Holtz, F., Roux, J., 1996. Water and the viscosity of andesite melts. Chemical Geolology 128, 185-197.

Richet, P., Lejeune, A.M., Holtz, F., Roux, J., 2000. Water and density of silicate glass. Contributions to Mineralogy and Petrology 138, 337-347.

Romano, C., Poe, B., Mincione, V., Hess, K.U., Dingwell, D.B., 2001. The viscosities of dry and hydrous $XAlSi_3O_8$ (X = Li, Na, K, $Ca_{0.5}$, $Mg_{0.5}$) melts. Chemical Geology 174, 115-132.

Roscoe, R., 1952. The viscosity of suspensions of rigid spheres. British Journal of Applied Physics 3, 267–269.

Russell, J.K., Girdano, D. and Dingwell D.B. 2003. High-temperature limits on viscosity of non-Arrhenian silicate melts. American Mineralogist 88, 1390-1394.

Sato, H., 2005. Viscosity measurements of subliquidus magmas:1707 basalt of Fuji volcano. Journal Mineralogy and Petrology Science 100, 133-142.

Schulze, F., Behrens, H., Holtz, F., Roux, J., Johannes, W., 1996. The influence of H_2O on the

viscosity of a haplogranitic melt. Am. Mineral. 81, 1155-1165.

Schulze, F., Behrens, H., Hurkuck, W., 1999. Determination of the influence of pressure and dissolved water on the viscosity of highly viscous melts: Application of a new parallel-plate viscometer. American Mineralogist 84, 1512-1520.

Shaw, H.R., 1963. Obsidian-H_2O viscosities at 100 and 200 bars in temperature range 700 degrees to 900 degrees C. Journal of Geophysical Research 68 (23), 6337-6343.

Shaw, H.R., 1972. Viscosities of magmatic silicate liquids - Empirical method of prediction. American Journal Science 272, 870-893.

Sparks, R.S.J., Baker, L., Brown, R.J., Field, M., Schumacher, J., Stripp, G., Walters, A., 2006. Dynamical constraints on kimberlite volcanism. Journal of Volcanology and Geothermal Research 155, 18-48.

Ventura, G., Vilardo, G., Milano, G., Pino, N.A., 1999. Relationships among crustal structure, volcanism and strike-slip tectonics in the Lipari-Vulcano volcanic complex (Aeolian Islands, Southern Tyrrhenian Sea, Italy). Physics of the Earth Planetary Interior 116, 31-52.

Vetere, F., Behrens, H., Holtz, F., Neuville, D., 2006. Viscosity of andesitic melts – new experimental data and a revised calculation model. Chemical Geology 228, 233-245.

Vetere, F., Behrens, H., Schuessler J.A., Holtz F., Valeria Misiti , L. Borchers, 2007. Viscosity of andesite melts and its implication for magma mixing prior to Unzen 1991-1995 eruption. Journal of Volcanology and Geothermal Research, Unzen special issue, accepted.

Whittington, A., Richet, P., Holtz, F., 2000. Water and the viscosity of depolymerized aluminosilicate melts. Geochimica et Cosmochim. Acta 64, 3725-3736.

Wilson, A. D., 1960. The micro-determination of ferrous iron in silicate minerals by a volumetric and colorimetric method. Analyst 85, 823-827.

Wylie, J.J., Helfrich, K.R., Dade, B., Lister, J.R., Salzig, J.F., 1999. Flow localization in fissure eruptions. Bulletin of Volcanology 60, 432–440.

Zanon, V., Frezzotti, M.L., Peccerillo, A., 2003. Magmatic feeling system and crustal magma accumulation beneath Vulcano Island (Italy): evidence from CO_2 fluid inclusions in quartz xenoliths. Journal of Geophysical Research 108, B6,2298

Zhang, Y., Xu, Z.J., Liu, Y., 2003. Viscosity of hydrous rhyolitic melts inferred from kinetic experiments, and a new viscosity model. American Mineralogist 88, 1741-1752.

Zietka, S., Deubener, J., Behrens, H., Muller, R.. Glass transition and viscosity of hydrated silica

glasses. European Journal of Glass Science and Technology Part B Physics and Chemistry of Glasses. In press

Figure caption

Fig. 1. a) Geological sketch map of Vulcano island (modified from De Astis et al., 1997); b) Detail of the Vulcanello peninsula.

Fig. 2. Back scattered images of samples Vul6 and Vul8 obtained at 1473 K. Note the increase of crystals content as pressure increase from 500 (Vul6) to 2000 (Vul8) MPa.

Fig. 3. Low temperature viscosity data for dry and hydrous samples indicating near-Arrhenian behaviour of the shoshonitic melts in the high viscosity range.

Fig. 4. Typical dataset produced during a micropenetration experiment (sample Vul y_1, Table 3): viscosity, temperature and indentation of the sphere vs time. Note the relative increase in viscosity during running time.

Fig. 5. Comparison between determined viscosity data obtained for a shoshonitic melt and the predicted viscosity using the empirical model (equation 5).

Fig. 6. Comparison of the viscosity of a nearly anhydrous shoshonitic melt with models predicting the viscosity of a nearly anhydrous basalt, andesite and trachyte (see compositions in Table 1).

Figure

Fig.1

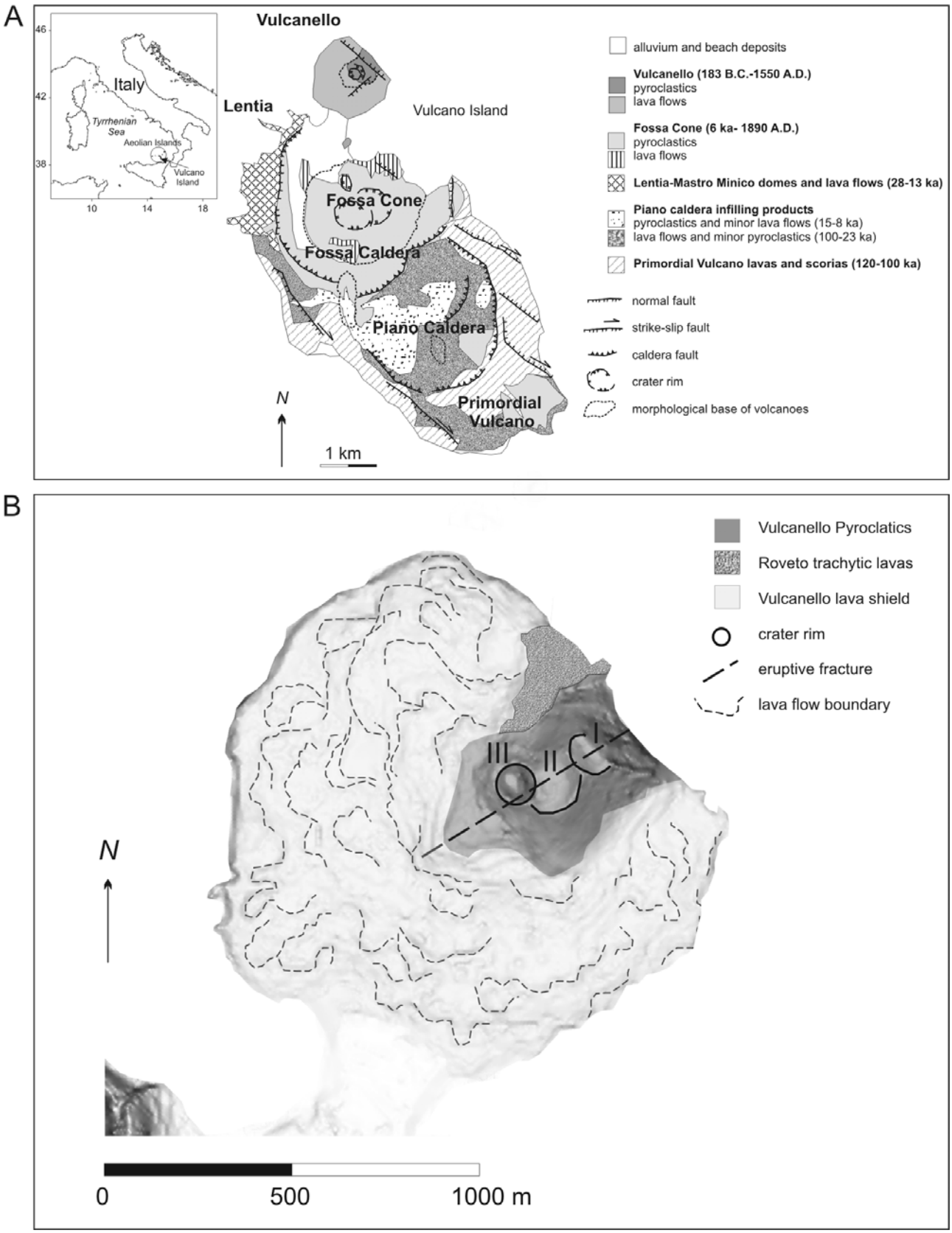
A
Vulcanello
Lentia
Vulcano Island
Fossa Cone
Fossa Caldera
Piano Caldera
Primordial Vulcano
N
1 km
Italy
Tyrrhenian Sea
Aeolian Islands
Vulcano Island
46
42
38
10
14
18
alluvium and beach deposits
Vulcanello (183 B.C.-1550 A.D.)
pyroclastics
lava flows
Fossa Cone (6 ka- 1890 A.D.)
pyroclastics
lava flows
Lentia-Mastro Minico domes and lava flows (28-13 ka)
Piano caldera infilling products
pyroclastics and minor lava flows (15-8 ka)
lava flows and minor pyroclastics (100-23 ka)
Primordial Vulcano lavas and scorias (120-100 ka)
normal fault
strike-slip fault
caldera fault
crater rim
morphological base of volcanoes
B
Vulcanello Pyroclatics
Roveto trachytic lavas
Vulcanello lava shield
crater rim
eruptive fracture
lava flow boundary
III
II
I
N
0
500
1000 m

Fig. 2

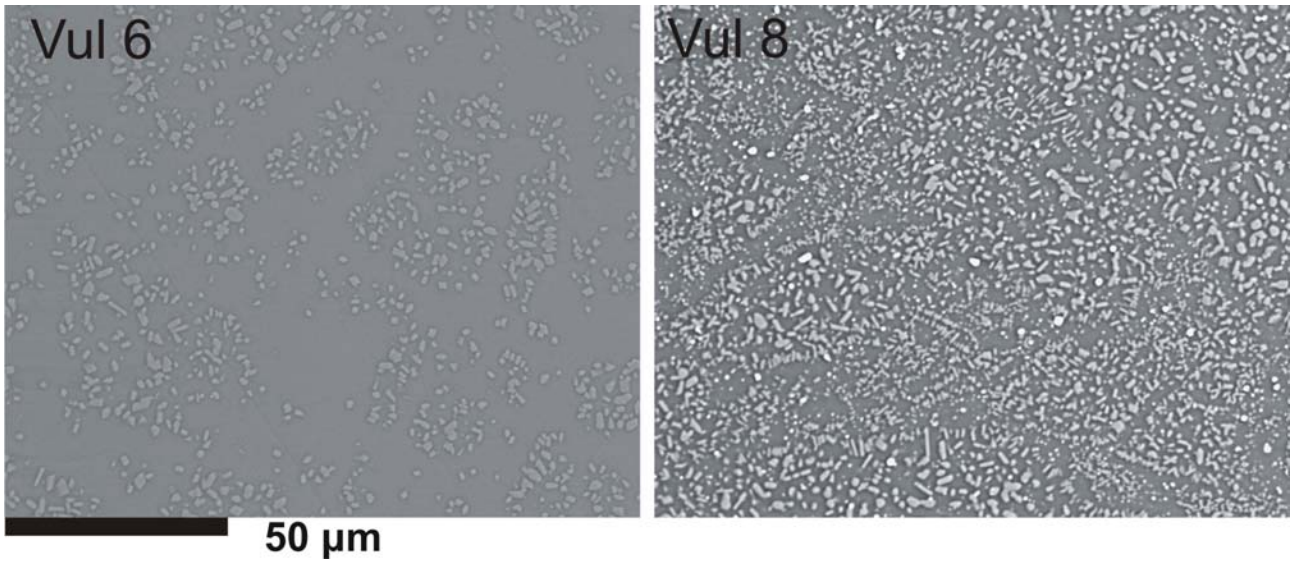

Fig 3

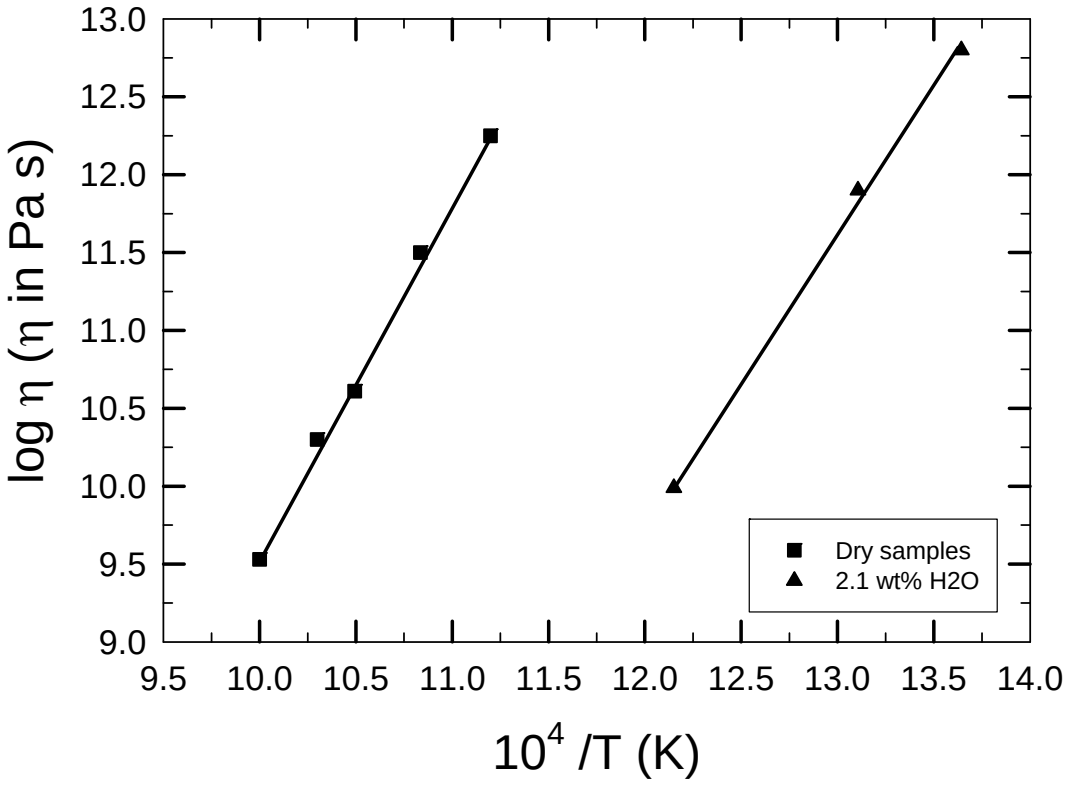
log η (η in Pa s)
13.0
12.5
12.0
11.5
11.0
10.5
10.0
9.5
9.0
9.5
10.0
10.5
11.0
11.5
12.0
12.5
13.0
13.5
14.0
10^4 /T (K)
Dry samples
2.1 wt% H2O

Fig.4

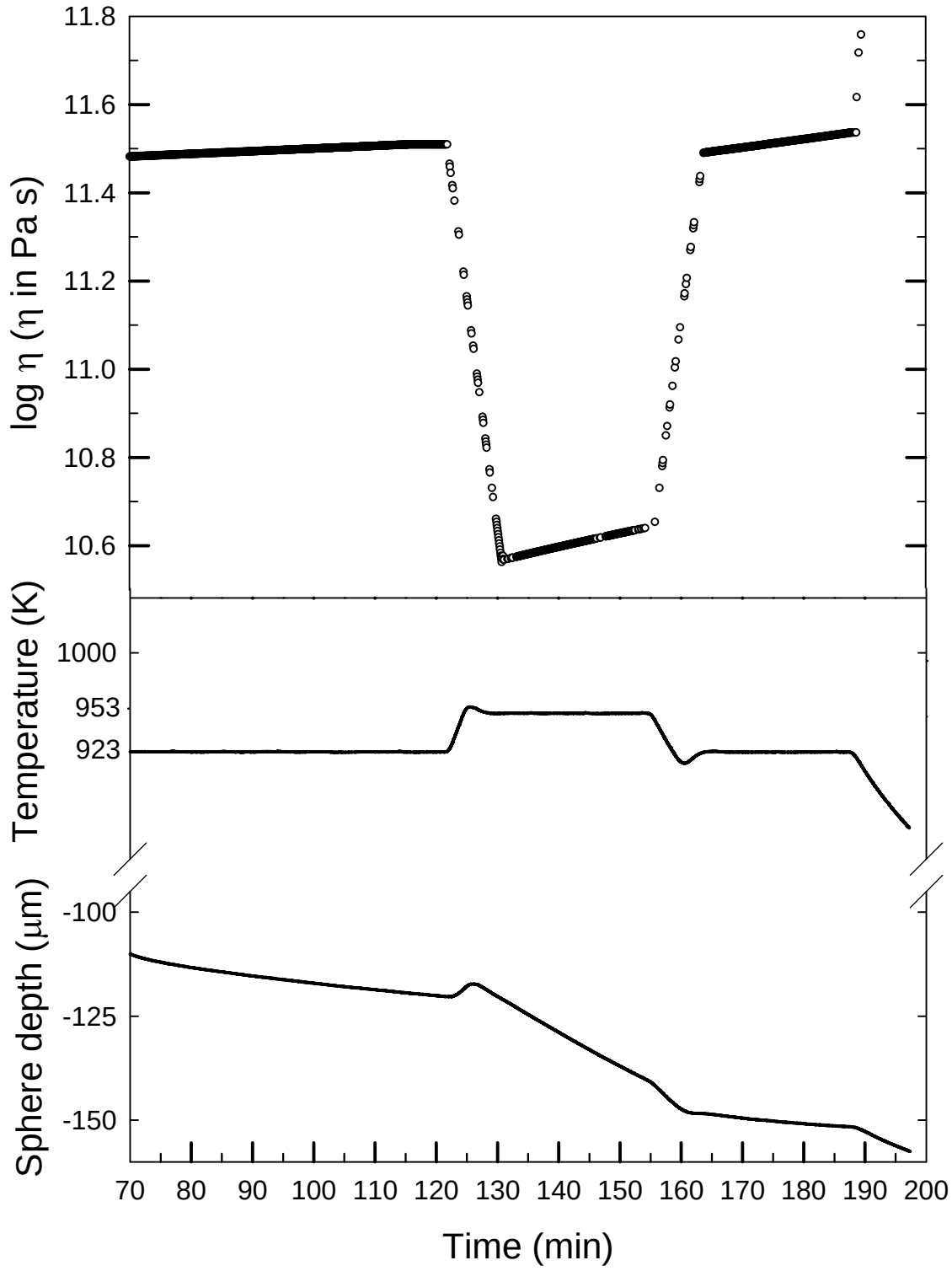
log η (η in Pa s)
11.8
11.6
11.4
11.2
11.0
10.8
10.6
Temperature (K)
1000
953
923
Sphere depth (μm)
-100
-125
-150
70
80
90
100
110
120
130
140
150
160
170
180
190
200
Time (min)

Fig 5

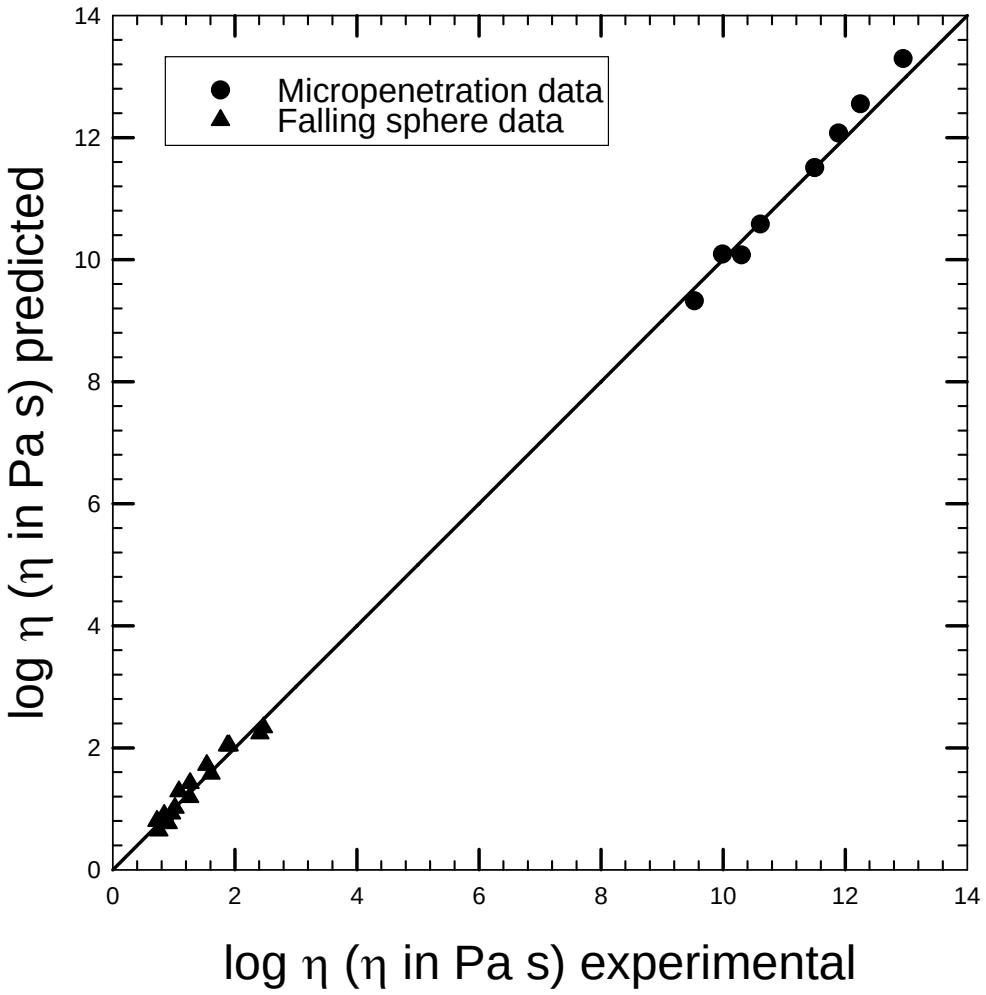
Micropenetration data
Falling sphere data
log η (η in Pa s) predicted
log η (η in Pa s) experimental
0
2
4
6
8
10
12
14

FIG 6

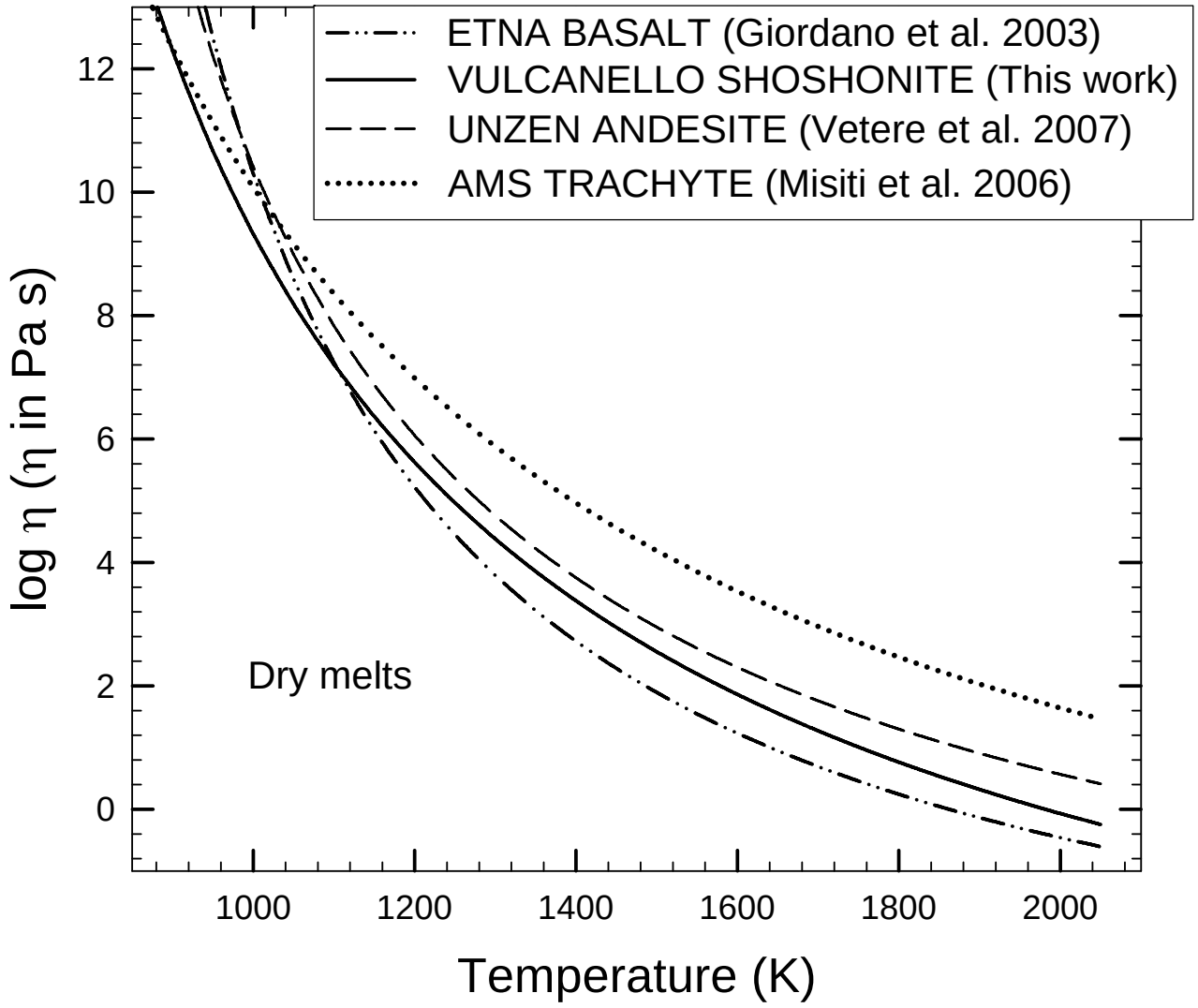
ETNA BASALT (Giordano et al. 2003)
VULCANELLO SHOSHONITE (This work)
UNZEN ANDESITE (Vetere et al. 2007)
AMS TRACHYTE (Misiti et al. 2006)
Dry melts
log η (η in Pa s)
Temperature (K)
0
2
4
6
8
10
12
1000
1200
1400
1600
1800
2000

Table 1. Electron microprobe analyses and water content of the starting material in comparison to basalt and andesite and trachyte (wt%).

	Shoshonite	Etna basalt [a)]	Unzen andesite[b)]	AMS trachyte[c)]
SiO_2	53.47 (0.29)	48.02	55.11 (0.44)	59.90
TiO_2	0.03 (0.07)	1.64	1.09 (0.05)	0.39
Al_2O_3	15.48 (0.20)	16.63	18.39 (0.36)	18.00
FeO_{tot} [d)]	8.39 (0.33)	-	9.16 (0.32)	3.86
FeO	-	3.41	-	-
Fe_2O_3	-	7.70	-	-
MnO	0.16 (0.10)	0.20	0.08 (0.06)	0.12
MgO	4.88(0.17)	5.28	2.88 (0.17)	0.89
CaO	8.51 (0.25)	10.69	8.44 (0.25)	2.92
Na_2O	3.66 (0.15)	3.83	3.38 (0.25)	4.05
K_2O	4.72 (0.16)	1.98	1.41 (0.08)	8.50
P_2O_5	-	0.60	-	0.21
Fe^{2+}/Fe_{tot} [e)]	0.40	-	0.41	-
H_2O (IR)	0.029	-	0.015	-

Notes. Compositions are normalized to a total of 100 wt%. Numbers in parentheses correspond to 1 σ standard deviation. H_2O contents were measured by IR spectroscopy using the peak height of the absorption band at 3550 cm^{-1}.

[a)] Basaltic lava from the 1992 flow at Etna, Italy; Giordano and Dingwell (2003).

[b)] Andesite from Unzen vulcano, Japan; Vetere et al. (2007).

[c)] AMS trachyte used for viscosity determination in Misiti et al (2006).

[d)] Total iron is given as FeO.

[e)] Fe^{2+}/Fe_{tot} was measured using the modified Wilson method (see text).

Table 2 Experimental conditions and results of viscosity experiments using the falling sphere method.

No.	Apparatus	H_2O initial (wt%)	H_2O final (wt%)	Pressure (MPa)	T (K)	Sphere radius (μm)	C_f	Dwell time (s)	Effective time (s)	Falling distance (cm)	η (Pa·s)	Fe^{2+}/Fe_{tot} before exp.	Fe^{2+}/Fe_{tot} after exp.
Vul 3 §)	PCA	0.03		500	1473	90±2.5 Pt	0.87	7198	7225	0.268	891.3±101.5		
Vul 4 §)	PCA	0.03		500	1473	95±2.5 Pt	0.88	7198	7225	0.292	812.8±91.4		
Vul 5 §)	PCA	0.03		500	1473	150±5 Pt	0.79	3595	3622	0.276	955.0±114.3	0.55	
Vul 6 §)	PCA	0.03		500	1473	95±2.5 Pt	0.88	10798	10825	0.283	1122.0±126.2	0.56	
Vul 8 #)	PCA	0.03		2000	1473	175±5 Pt	0.79	3597	3624	0.111	3252.8±373.1	0.57	
Vul 23a	PCA	0.03		500	1573	95±5 Pt	0.93	700	729	0.332	75.9±7.6		
Vul 23b	PCA	0.03		500	1573	125±2.5Pd	0.93	1800	1828	0.541	72.2±6.8		
Vul 7	PCA	0.03		2000	1573	90±2.5 Pt	0.94	697	726	0.281	80.6±8.2		
Vul 22	PCA	0.03		500	1623	90±2.5 Pt	0.94	700	731	0.659	34.8±3.4		
Vul 21	PCA	0.03		500	1673	120±5 Pt	0.92	250	282	0.829	18.5±2.2	0.66	0.68
Vul 15	IHPV	0.58	0.62	500	1473	185±5 Pt	0.92	3500	3645	1.571	294.3±33.3	0.75	0.74
Vul 27	PCA		2.04^t	500	1373	185±5 Pt	0.93	700	725	0.311	258.1±33.8		
Vul 25	PCA	2.01^b-1.98^t		500	1473	67.5±2.5	0.95	700	727	0.317	40.9±5.1		
Vul 24	PCA	2.01		500	1523	72.5±2.5Pd	0.95	700	728	0.637	12.1±1.4	0.73	
Vul 28	PCA		2.01^b	500	1573	85±2.5Pd	0.94	500	528	0.701	10.5±1.1		0.74
Vul 17a	IHPV	3.08^t-2.96^b		500	1473	70±2.5 Pt	0.98	360	405	0.442	18.1±2.3	0.68	
Vul 17b	IHPV		3.10^c	500	1523	70±2.5 Pt	0.98	600	647	1.382	9.2±1.1		0.70
Vul 2	IHPV	3.68^t-3.62^b	3.70^t	500	1523	65±1	0.98	240	287	0.602	8.1±0.8	0.57	0.56
Vul 13a	IHPV	4.27		500	1473	62.5±1 Pt	0.98	360	405	0.910	6.9±0.7	0.61	0.64
Vul 13b	IHPV		4.19	500	1523	62.5±1 Pt	0.98	240	287	0.791	5.6±0.6		
Vul 16	IHPV	4.75		500	1473	54±1 Pt	0.98	360	405	0.902	5.3±0.6		

Notes. Experiments using same sample are presented in the order in which they were performed (labeled as a and b in the sample name). Sphere radii were determined before incorporation in the glass. C_f refers to the Faxen correction. Nominally dry samples were analyzed by IR spectroscopy, hydrous samples (>0.5 wt% H_2O) were analyzed by KFT. Superscript t, b and c refer to top, bottom and center part of the sample, the location where samples for KFT analysis was taken. §) Samples contain ~11 vol % of crystals. #) Sample contain ~24 vol% of crystals.

Table 3. Results of micropenetration viscometry at 1 atm.

Sample	Temperature (K)	log η (Pa·s)	Load (g)	H_2O (wt%)
Vul y_1	923	11.50	800	0.019^{IR}
	953	10.61		
Vul y_2	893	12.25	900	0.030^{IR}
	971	10.30		
	1003	9.53		
Vul 14	823	9.99	500	2.11^{KFT}
	733	12.80		
	763	11.89		

Note: The superscript IR refers to infrared and the subscript KFT refers to Karl-Fischer titration. Experiments on the same sample are presented in the order in which they were performed.